Experimental Thermal and Fluid Science 98 (2018) 278–289

Contents lists available at ScienceDirect

Experimental Thermal and Fluid Science

journal homepage: www.elsevier.com/locate/etfs

Bubble convection and bubbly flow turbulent time and length scales in two-dimensional plunging jets

Rui Shi, Hang Wang*, Hubert Chanson

The University of Queensland, School of Civil Engineering, Brisbane, QLD 4072, Australia

ARTICLE INFO

Keywords:
Plunging jet
Air entrainment
Bubble clustering
Integral turbulent scales
Schmidt number

ABSTRACT

Air entrainment and air-water mixing by a flow impingement are enhanced by the turbulent shear layer and associated instabilities in the receiving waterbody. This paper presents an experimental study aiming at a quantitative description of bubble-turbulence interplay in two-dimensional supported plunging water jets. In addition to the basic air-water flow properties, the turbulence intensity in the highly-aerated plunging pool was estimated based on void fraction and total pressure fluctuation measurements, while the turbulent time and length scales were recorded systematically. The coupling of bubble convection and formation of macroscopic turbulent structures was characterised in terms of bubble clustering behaviours and turbulent length and time scales of the bubbly flow eddy structures. The effects of jet impact velocity were investigated for a fixed jet length. These advanced data analyses were applied to plunging jet two-phase flow for the first time. The results would provide new benchmark data for numerical modelling of intense air-water flow at a higher level than the basic two-phase flow dynamic properties. A discussion was developed at the end on the turbulent length scales and the Schmidt number in the bubbly flow regions of horizontal hydraulic jump and vertical supported plunging jet.

1. Introduction

Air-water two-phase flow is a major concern in the study and application of mass and heat transfer because it induces substantial change in interfacial area [1,2]. Self-sustained air entrainment into water may be achieved by inducing free-surface breaking. A canonical case is a plunging jet, where air is entrained at the intersection between the impinging jet and receiving bath [3,4]. The impingement point is a discontinuity in free-surface profile, velocity and pressure fields. In addition to the source of aeration, it also acts as the origin of a turbulent shear layer between the high-speed jet core and the ambient water in the receiving pool [5]. The development of turbulent instabilities enhances the air entrainment and bubble convection, and large entrained air bubbles are broken into small ones by the turbulent shear forces, enlarging significantly the air-water interfacial area. The mass and heat transfer is also enhanced by the increase in submerged bubble lifetime associated with the longer advection distance and recirculating motion. The presence of air bubbles further modifies the turbulence field by bubble deformation, thus influencing the energy dissipation. A prerequisite for the understanding of all these physical processes is a quantitative description and interpretation of the bubble-turbulence interplay.

To date, the most reliable method to investigate air-water open channel flow at high Reynolds numbers is still physical modelling, and successful measurement techniques include flow imaging and intrusive phase detection [6,7]. Although numerical simulation has the potential to provide detailed flow characterisation, the model must be verified at a proper level [8,9]. For example, a numerical prediction of eddy lifetime cannot only be verified using the time-averaged void fraction or velocity distributions, but also has to involve experimentally-quantified turbulent time scale data [10,11]. A recent numerical study of hydraulic jump by Mortazavi et al. [12] presented for the first time the model verification using the integral turbulent length scale. For plunging jet flows, most literature on air-water flow measurement focused on basic two-phase flow properties such as void fraction, air- or water-phase velocity, air entrainment rate, bubble size, penetration depth, etc., with few attempts at turbulence measurement [13–18]. There is basically no benchmark data that quantify the bubble-turbulence interaction in detail.

The present study presented an attempt to measure the bubbly flow structures in highly-aerated plunging jets. The quantitative parameters adopted to describe the coupling between bubble convection and flow turbulence included the bubble clustering properties and characteristic turbulent length and time scales, which were applied to plunging jets

* Corresponding author.
E-mail address: hang.wang@uqconnect.edu.au (H. Wang).

https://doi.org/10.1016/j.expthermflusci.2018.06.008
Received 8 December 2017; Received in revised form 12 April 2018; Accepted 11 June 2018
Available online 12 June 2018
0894-1777/

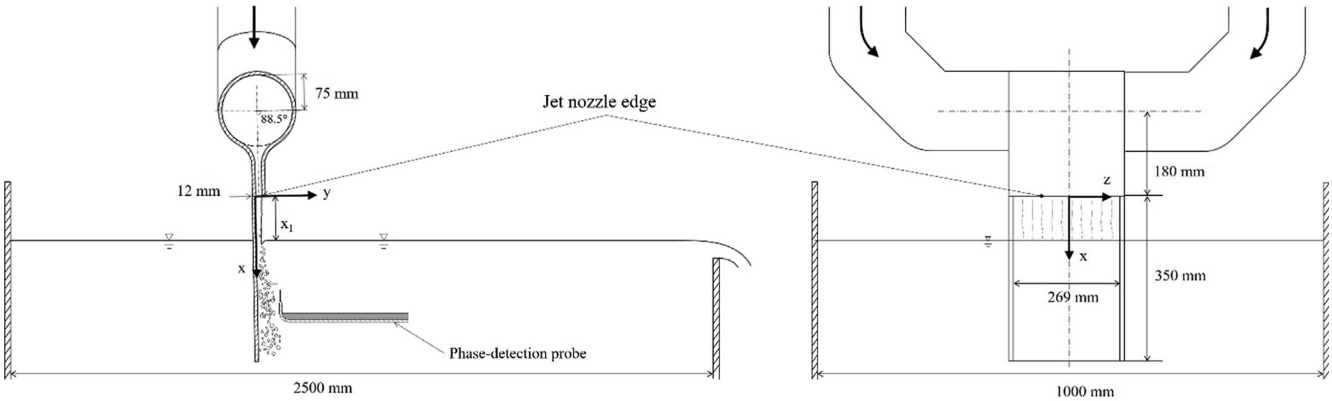

Fig. 1. Definition sketch of planar plunging jet experimental setup: side view (left) and front view (right).

for the first time. The measurements were conducted using a series of intrusive conductivity phase-detection probes. The key results are presented after basic characterisation of the air-water flow, followed by a comparative discussion on the turbulent length scale data in horizontal hydraulic jump and vertical supported plunging jet.

2. Experimental facility and instrumentation

The experimental facility consisted of a rectangular jet nozzle and a receiving water tank. The jet nozzle was 0.269 m wide, with a 0.012 m opening that equalled to the initial jet thickness d_0. A quasi-two-dimensional planar water jet was discharged downwards into a 2.5 m long, 1 m wide, 1.5 m deep receiving bath. The planar jet was supported on one side by a full-width PVC sheet extending 0.35 m from the nozzle edge. The jet support was built with transparent sidewalls that constrained the falling jet within the width of the support and enabled flow visualisation. The jet nozzle and support system was set to 88.5° from the horizontal to prevent jet detachment. The large-size receiving water tank ensured the air-water flow in the plunging pool free of boundary effects. A sharp-crested weir at the far end of the tank allowed for a constant water level control during the experiments. Fig. 1 shows a sketch of the experimental system, where the longitudinal coordinate x originated from the nozzle edge and the normal coordinate y (perpendicular to the jet support) from the jet support plane.

The water discharge was measured with an orifice or Venturi meter that was calibrated onsite, with expected percentage of error within ± 2%. A mass conservation check based on velocity and void fraction measurements in the falling jet confirmed adequate accuracy of the flow rate measurement. Two fine-adjustment travelling mechanisms were used to control the translation of flow-measuring probes in the longitudinal and normal directions. The probe position was read from two linear position sensors that provided accuracy within 0.05 mm.

The air-water flow properties were measured using a series of dual-tip phase-detection probes. Each probe had two phase-detection needle sensors that were mounted parallel to each other and both against the flow direction, with a difference Δx in sensor length. Each needle sensor detected air-water interfaces on the sensor tip based on the change in electrical conductivity of air and water phases between the central electrode (Ø = 0.25 mm) and the outer electrode (Ø = 0.80 mm) of the sensor. Both sensors were sampled simultaneously at 20 kHz for 90 s at each measurement location. A total of six dual-tip phase-detection probes with different Δx = 2.4 mm, 4.9 mm, 7.1 mm, 9.9 mm, 16.0 mm and 25.0 mm were used to enable measurements of integral turbulent length and time scales (see Section 3.4).

For a number of experiments, a total pressure probe was mounted side by side to the phase-detection probe to quantify the turbulence intensity in the bubbly flow (see Section 3.2). The pressure sensor had a 5 mm external diameter with a 1 mm diameter silicon diaphragm detecting the instantaneous stagnation pressure. The absolute pressure measurement range was 0–1.5 bars. The centre of the pressure sensor head was at the same longitudinal and normal positions as the phase-detection probe leading tip, with a transverse separation of 6.2 mm. The total pressure sensor was sampled simultaneously with the phase-detection probe at 20 kHz.

3. Data processing

3.1. Basic air-water flow properties

The individual bubble detection was analysed using the binarised phase-detection signal, where a 50% threshold between the maximum possibilities of air and water phases was adopted. Voltage samples above the threshold were converted to an instantaneous void fraction of 0 in water, and those below the threshold were converted to a void fraction of 1 in air. The binarised signal provided the local time-averaged void fraction and bubble count rate within the sampling duration. The results presented in this paper are the ensemble-averaged values of six phase-detection probes.

3.2. Velocity and turbulence intensity

The velocity of air-water interfaces in high-speed bubbly flow was found to be very close to the flow velocity, and the non-slip condition held [19,20]. The interfacial velocity was measured between the two phase-detection sensor tips aligned in the longitudinal direction. A cross-correlation between the sensor signals showed a maximum correlation coefficient $R_{xy,max}$ at a time lag T, and the longitudinal interfacial velocity equalled to

$$V = \frac{\Delta x}{T} \tag{1}$$

Δx being the longitudinal separation distance between the sensor tips. The longitudinal velocity component is deemed to be equal to the interfacial velocity in the jet core region.

The velocity fluctuations were derived from total pressure measurement in the bubbly flow, assuming a negligible static pressure fluctuation. The density variation associated with the discontinuous two-phase flow was approximated using the local void fraction measured simultaneously beside the total pressure measurement location. Neglecting the higher order terms, the turbulence intensity Tu was calculated as [21]

$$Tu = \sqrt{\frac{\frac{p_t'^2}{\rho_w^2 V^4} - \frac{(1-C)C}{4}}{(1-C)\left(1+\frac{C}{2}\right)}} \tag{2}$$

where Tu is defined as v′/V, v′ is the velocity standard deviation, V is